Journal of Solid State Chemistry 184 (2011) 1472–1477

Contents lists available at ScienceDirect

Journal of Solid State Chemistry

journal homepage: www.elsevier.com/locate/jssc

Two highly proton-conductive molecular hybrids based on ionized water clusters and poly-Keggin-anion chains

Mei-Lin Wei*, Peng-Fei Zhuang, Qiu-Xiang Miao, Yan Wang

College of Chemistry and Environmental Science, Henan Normal University, Xinxiang 453007, China

ARTICLE INFO

Article history:
Received 25 November 2010
Received in revised form
5 April 2011
Accepted 10 April 2011
Available online 20 April 2011

Keywords:
Polyoxometalates
Structure elucidation
Organic–inorganic hybrid composites
Conducting materials

ABSTRACT

Two proton-conductive molecular hybrid complexes, $\{[Zn(H_2O)_8][H(H_2O)_2](HINO)_4(PMo_{12}O_{40})\}_n$ (**1**) and $\{[Mn(H_2O)_8][H(H_2O)_{2.5}](HINO)_4(PMo_{12}O_{40})\}_n$ (**2**), were constructed by introducing protonated water clusters, transition metal ionized water clusters and $[PMo_{12}O_{40}]^{3-}$ anions in the gallery of H-bonding networks based on isonicotinic acid N-oxide (HINO). Single-crystal X-ray diffraction analyses at 293 K revealed that both complexes presented exactly the same three-dimensional (3D) hydrogen-bonded networks with large one-dimensional (1D) channels. Interestingly, $[PMo_{12}O_{40}]^{3-}$ anions just filled in the 1D channels and self-assembled into poly-Keggin-anion chains. Thermogravimetric analyses both show no weight loss in the temperature range of 20–100 °C, indicating that all water molecules in the unit structure are not easily lost below 100 °C. Surprisingly, the proton conductivities of **1** and **2** in the temperature range of 85–100 °C under 98% RH conditions reached high proton conductivities of 10^{-3} S cm^{-1}. A possible mechanism of the proton conduction was proposed according to the experimental results.

1. Introduction

Keggin-type heteropolyacids (HPAs), possessing a unique discrete ionic structure including heteropolyanions and countercations (H^+, H_3O^+, $H_5O_2^+$, etc.), are widely known as proton conducting electrolytes for low-temperature hydrogen–oxygen fuel cells [1]. However, the application of HPAs is limited by the extreme sensitivity of their conductivity to the relative humidity (RH) and the temperature of the surrounding atmosphere [2]. To overcome these problems, various attempts have been made to immobilize HPAs in silica gel and to disperse it in an organically modified electrolyte membrane and organic/inorganic hybrid membranes [3,4]. In addition, to enable fast ionic conduction in the hybrid materials, the molecular modification of organic ligand to inorganic structures of HPAs has been continuously investigated [5]. For a long time, we have focused on the proton conductivity of organic/inorganic complexes based on the transition metal salts of HPAs dispersing in self-ordered hydrogen-bonding (H-bonding) networks. In this work, we have succeeded in constructing two proton-conductive organic/inorganic complexes by introducing protonated water clusters, transition metal ionized water clusters and $[PMo_{12}O_{40}]^{3-}$ anions in the gallery of H-bonding networks constructed by isonicotinic acid N-oxide (HINO). Here, we report their syntheses, crystal structures and proton conductivities as a function of temperature.

2. Experimental

2.1. Materials and instruments

All organic solvents and material used for synthesis were of reagent grade and used without further purification. α-$H_3PMo_{12}O_{40}\cdot 6H_2O$ was prepared according to a literature method [6] and characterized by IR spectra and TG analyses. HINO was synthesized according to a literature method [7] and characterized by IR spectra. Elemental analyses (C, H, and N) were carried out on a Perkin-Elmer 240C analyzer. X-ray powder diffraction (XRD) was performed on a Bruker D8 Advance Instrument using Cu$K\alpha$ radiation and a fixed power source (40 kv, 40 mA). IR spectra were recorded on a VECTOR 22 Bruker spectrophotometer with KBr pellets in the 400 – 4000 cm^{-1} region at room temperature. Thermogravimetric analysis was performed on a Perkin-Elmer thermal analyzer under nitrogen at a heating rate of 10 °C min^{-1}. For an electrical conductivity study, the powdered crystalline samples were compressed to 0.7 – 1.0 mm in thickness and 12.0 mm in diameter under a pressure of 12 – 14 MPa. ac Impedance spectroscopy measurement was performed on a chi660b (Shanghai chenhua) electrochemical impedance analyzer with copper electrodes [8] (the purity of Cu is more than 99.8%) over the frequency range from 10^5 to 10 Hz.

* Corresponding author. Fax: +86 373 3329281.
E-mail address: weimeilinhd@163.com (M.-L. Wei).

0022-4596/$ - see front matter © 2011 Elsevier Inc. All rights reserved.
doi:10.1016/j.jssc.2011.04.025

Samples were placed in a temperature–humidity controlled chamber (GT-TH-64Z, Dongwan Gaotian Corp.) The conductivity was calculated as $\sigma=(1/R)\times(h/S)$, where R is the resistance, h is the thickness, and S is the area of the tablet.

2.2. Synthesis of complex 1

The formation of heteropolyacid manganese salts was accomplished by neutralization of the acids. α-$H_3PMo_{12}O_{40}\cdot 6H_2O$ (120 mg, 0.06 mmol) and adding $ZnCl_2$ (9 mg, 0.06 mmol) dissolved in water (4 ml). The solution was heated at 80 °C in a water bath. Yellow crystals were formed by cooling the saturated solution and slow evaporation at room temperature, and characterized by IR spectrum. A mixture of result heteropolyacid zinc salts (60 mg, 0.03 mmol) and HINO (17 mg, 0.12 mmol) dissolved in enough acetonitrile/water (1:1, v/v) solution. Finally, the solution was filtered and left to evaporate at room temperature. Four or five days later, yellow crystals appeared and were collected and dried in air after quickly being washed with water. Yield: 51.6 mg, 86% based on α-$H_3PMo_{12}O_{40}\cdot 6H_2O$. Anal. calcd (%) for $C_{24}H_{41}N_4O_{62}ZnMo_{12}P$: C, 10.98; H, 1.58; N, 2.13; Found (%): C, 10.90; H, 1.64; N,2.15. IR (KBr) ν, cm^{-1}: four characteristic vibrations resulting from heteropolyanions with the Keggin structure: 803 ν(Mo–O_c) , 878 ν(Mo–O_b), 961 ν(Mo=O_t), 1065 ν(P–O_a); and another vibrations resulting from the HINO molecules: 3326 ν(O–H), 1697 ν(C=O), 1618 ν(C=C),1204 ν(N–O) , 1168 δ(C–H, in plane).

2.3. Synthesis of complex 2

Complex **2** was prepared in the same way as for **1**, except using $MnCl_2\cdot 4H_2O$ (12 mg, 0.06 mmol) to replace $ZnCl_2$. Yield: 51.0 mg, 85% based on α-$H_3PMo_{12}O_{40}\cdot 6H_2O$. Anal. calcd (%) for $C_{24}H_{42}N_4O_{62.5}MnMo_{12}P$: C, 10.98; H, 1.61; N, 2.13; Found (%): C, 10.91; H, 1.64; N,2.19. IR (KBr) ν, cm^{-1}: four characteristic vibrations resulting from heteropolyanions with the Keggin structure: 802 ν(Mo–O_c), 879 ν(Mo–O_b), 961 ν(Mo=O_t), 1064 ν(P–O_a); and another vibrations resulting from the HINO molecules: 3326 ν(O–H), 1696 ν(C=O), 1618 ν(C=C),1203 ν(N–O) , 1169 δ(C–H, in plane).

2.4. Structure determination

Intensity data of **1** and **2** were collected on a Siemens SMART-CCD diffractometer with graphite-monochromated Mo$K\alpha$ radiation ($\lambda=0.71073$) using SMART and SAINT [9]. The structure was solved by direct methods and refined on F^2 by using full-matrix least-squares method with SHELXTL version 5.1 [10]. For **1** and **2**, all non-hydrogen atoms except solvent water molecules were refined anisotropically. Hydrogen atoms of organic molecules were localized in their calculated positions, and refined using a riding model. Hydrogen atoms of water molecules were not treated. The crystal parameters, data collection and refinement results for both complexes are summarized in Table 1.

Table 1
Crystallographic data and refinement parameters for complexes **1** and **2**.

	1	**2**
Empirical formula	$C_{24}H_{41}N_4O_{62}ZnPMo_{12}$	$C_{24}H_{42}N_4O_{62.5}MnPMo_{12}$
Mr	2625.23	2623.81
Crystal system	Orthorhombic	Orthorhombic
Space group	*Pnnm*	*Pnnm*
a/Å	10.3055(8)	10.2653(14)
b/Å	15.8867(11)	16.037(2)
c/Å	19.7140(14)	19.944(3)
V/Å^3	3227.6(4)	3283.2(8)
Z	2	2
D_c/g cm^{-3}	2.701	2.654
μ/mm^{-1}	2.768	2.549
F(0 0 0)	2516	2516
Refl. measured	15 590	15 596
Refl. unique	2939	2980
R_{int}	0.1093	0.1232
Refinement parameters	268	269
GOF on F^2	1.072	0.972
R_1/wR_2 [$I\geq 2\sigma(I)$]	0.0404/0.1117	0.0516/0.1373
R_1/wR_2 (all data)	0.0454/0.1155	0.0613/0.1442
$\Delta\rho_{(max)}$ and $\Delta\rho_{(min)}$, *e* Å^{-3}	1.645 and −1.424	1.362 and −2.131

3. Result and discussion

3.1. Structure description

Complexes **1** and **2** were synthesized by the reaction of $MHPMo_{12}O_{40}\cdot nH_2O$ and HINO at room temperature. They were characterized by single-crystal X-ray diffraction, infrared spectroscopy, TG and elemental analyses. X-ray diffraction analyses at 293 K revealed that both complexes crystallized in the orthorhombic space group *Pnnm*, exhibited very close unit cell parameters, and then presented exactly 3D H-bonding networks with large 1D channels constructed by HINO molecules, $[M(H_2O)_8]^{2+}$ (M=Zn for **1**,=Mn for **2**) and $H^+(H_2O)_m$ (m=2 for **1**,=2.5 for **2**) clusters. Interestingly, $[PMo_{12}O_{40}]^{3-}$ anions just filled in the 1D channels and self-assembled into poly-Keggin-anion chains. For clarity of the structural description of both complexes, the same labeling was used.

In $[M(H_2O)_8]^{2+}$ aqua-complex (Fig. 1a), the M^{2+} ion is placed in a symmetry center and located in a coordination octahedral environment built from six water molecules (two O(1 W), two O(2 W) and two O(3 W) centers), as well as two O(4 W) centers are dangled outside the coordination shell through short H-bonding interaction with the coordination water molecules O(3 W). Moreover, two O(3 W) and two O(2 W) centers are, respectively, crystallographically disordered into four symmetrical positions with each oxygen site half-occupied. In the $H^+(H_2O)_2$ (the proton added to balance the charge) (Fig.1b) [11], two water molecules, O(5 W) and O(6 W), formed a hexagon; and in the $H^+(H_2O)_{2.5}$ (Fig. 1c), the O(7 W) with the occupancy of 50% is placed in a symmetry center and located in a hexagonal environment built from two water molecules (O(6 W) and O(5 W) centers). In both water clusters, the O(5 W) molecule is crystallographically disordered into two symmetrical positions with each oxygen site half-occupied, and O(6 W) is crystallographically disordered into four symmetrical positions with each oxygen site quarter-occupied. It is far more difficult to experimentally establish the position of excess proton unambiguously for such a complex systems, since the presence of C–H vibrations of the ligand and solvent molecules, and the P–O, Mo–O vibrations of the anions all influence the observation of the IR signals of O–H vibrations related to the excess proton. X-ray diffraction analyses at 293 K revealed that the title complex crystallized in the orthorhombic space group *Pnnm*. Though the basic structure of the water cluster can be determined easily according to the result of the X-ray structure analysis, the X-ray structure is not refined at a level that can isolate the position of the hydrogens, and therefore cannot identify the position of the proton. The determination of the protonated water cluster is based on the stoichiometry, the crystal data and relative references. It was reported that based on high-resolution solid-state ^{1}H and ^{31}P NMR, there were at least three different states for protons of $H_3PW_{12}O_{40}\cdot nH_2O$ (i) protons present in highly hydrated samples, (ii) protonated water which is hydrogen-bonded to terminal oxygen, W=O$\cdots$H$^+(H_2O)_2$

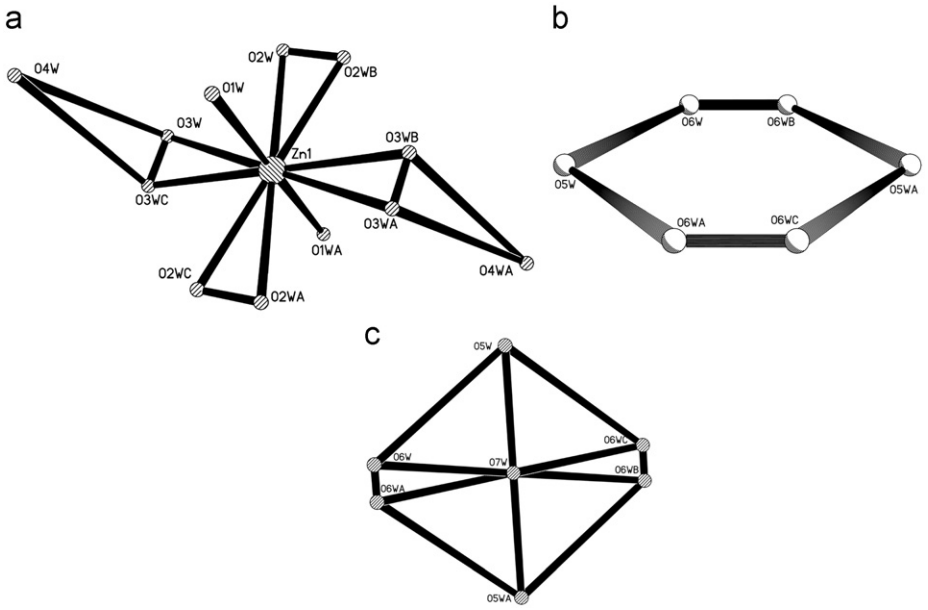

Fig. 1. Views of $[Zn(H_2O)_8]^{2+}$ (a), $H^+(H_2O)_2$ (b) and $H^+(H_2O)_{2.5}$ (c) clusters. Hydrogen atoms are omitted for clarity. Selected bond distances (Å) for complex **1**: Zn(1)–O(1 W) 2.065(6), Zn(1)–O(2 W) 2.025(8), Zn(1)–O(3 W) 2.067(8), O(4 W)···O(3 W) 2.599(2); for complex **2**: Mn(1)–O(1 W) 2.172(9), Mn(1)–O(2 W) 2.072(13), Mn(1)–O(3 W) 2.210(15), O(4 W)···O(3 W) 2.579(2).

(n=6), and (iii) proton which is directly bonded to bridging oxygen, W–OH–W(n=0) [12a]. More recently, it was reported that based on REDOR experiments acidic protons are localized on both bridging (O_c) and terminal (O_d) oxygen atoms of the Keggin unit in the anhydrous state of $H_3PW_{12}O_{40}$ [12b]. In title complexes, there are 2 or 2.5 lattice water molecules and the separations between them are enough short to stabilize the excess proton to form such an oligomer as $H_5O_2^+$, so, we think that the excess proton is not localized on the surface of the polyanion [11].

Interestingly, HINO molecules are not bound to the M^{2+} ion, but remaining outside the coordination shell to form H-bonding chains along the b-axis (Fig. 2). Two oxygen atoms O(15) and O(17) of each HINO molecule are involved in the H-bonding chains. As shown in Fig. 3, these HINO H-bonding chains are linked together by $[M(H_2O)_8]^{2+}$ aqua-complexes and small $H^+(H_2O)_m$ clusters into a 3D cationic network with large 1D channels through hydrogen bonds between coordination water molecules O(2 W) and oxygen atoms O(15) of HINO molecules, and between water molecules O(6 W) and oxygen atoms O(15), as well as through weak hydrogen bonds between coordination water molecules and oxygen atoms of HINO molecules. Thus, all O atoms of HINO are involved in the hydrogen bonds, creating a 3D supramolecular assembly with 1D channels. Moreover, there are H-bonding interaction between water molecules O(5 W) in the $H^+(H_2O)_m$ clusters and O(1 W) centers of the $[M(H_2O)_8]^{2+}$ cluster. The section size of the channels based on the M···M separations is ca. $10.3 \times 16.0 \times 19.8$ Å for **1** and $10.2 \times 15.9 \times 19.7$ Å for **2** (these separations are almost equal to three axial lengths, respectively), indicating that each pore could only accommodate a single Keggin anion. Interestingly, the M···M separation bridged by the $H^+(H_2O)_m$ clusters along the a-axis is much shorter than those separations along the b and c axes, and even shorter than the diameter of the discrete $[PMo_{12}O_{40}]^{3-}$ anion (ca. 10.4 Å), resulting in each cavity being heavily condensed along the a-axis. In addition, the presence of positively charged species, $[M(H_2O)_8]^{2+}$ and $H^+(H_2O)_m$ clusters, could attract the polyanions, as a result, the Keggin-type $[PMo_{12}O_{40}]^{3-}$ anions for charge compensation are embedded in the voids of the 3D cationic framework and connect

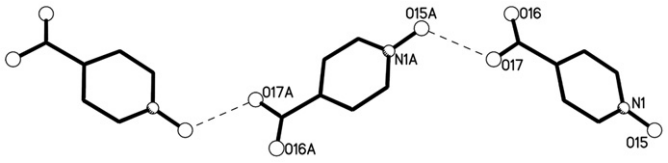

Fig. 2. View of the 1D HINOs chain along the b-axis. Hydrogen atoms are omitted for clarity. Selected atom···atom distances (Å) for complex **1**: O(17)···O(15 A) 2.626(2); for complex **2**: O(17)···O(15 A) 2.605(2). Symmetry code: A, $-x+5/2$, $y-1/2$, $-z+1/2$.

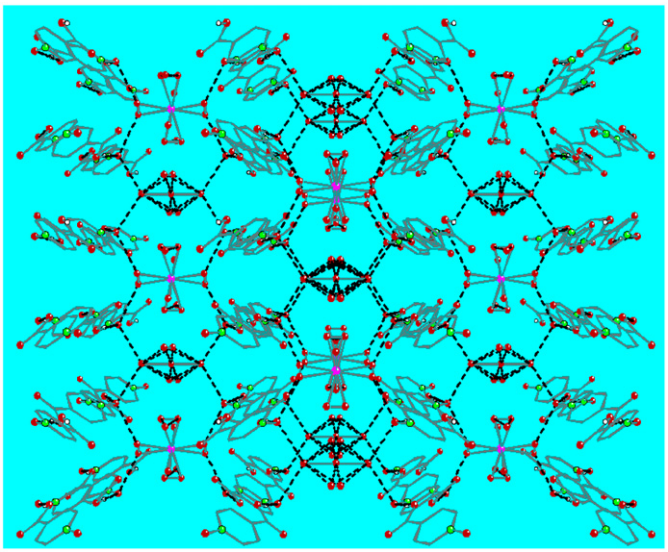

Fig. 3. Representative 3D hydrogen-bonded network constructed by HINO molecules, $[M(H_2O)_8]^{2+}$ and $H^+(H_2O)_m$ clusters. Zn(Mn), N and O are represented as purple, green and red, respectively. Hydrogen atoms are omitted for clarity. Selected atom···atom distances (Å) for complex **1**: O(1 W)···O(16 A) 3.012(2), O(2 W)···O(16 A) 2.945(2), O(3 W)···O(15B) 2.925(2); for complex **2**: O(1 W)···O(16 A) 2.942(2), O(2 W)···O(16 A) 2.952(3), O(3 W)···O(15B) 2.913(2) O(6 W)···O(1WC) 2.940(3). Symmetry code: A, $-x+3/2$, $y+1/2$, $-z+1/2$; B, $-x+1$, $-y-1$, $-z$; C, $-x-1$, $-y$, $-z-1$.

to one another leading to poly-Keggin-anion chains in the channel along the *a*-axis (Fig. 4). In the polymeric polyanion, there are some short atom···atom separations of 2.99(2) Å, such as O(7A)···O(8BB), O(8A)···O(7BB), O(7AA)···O(8CB), O(7CB)···O(8AA).

In the $[PMo_{12}O_{40}]^{3-}$ unit, the central P atom is surrounded by a cube of eight oxygen atoms with each oxygen site half-occupied. These eight oxygen atoms are all crystallographically disordered, and this case can be found in many compounds [11]. In complex **1**, the bond lengths of P–O and Mo–O are 1.518(9)–1.526(9) and 1.648(7)–2.484(9) Å, respectively; in complex **2**, the bond lengths of P–O and Mo–O are 1.525(11)–1.527(10) and 1.640(8)–2.475(10) Å, respectively. The bond lengths of P–O and Mo–O in two complexes are, respectively, comparable to those in the 3D porous polyoxometalates-based organic–inorganic hybrid materials with Keggin anions as guests [11]. In addition, the O–P–O angles are in the range of 109.0(5)–110.1(5)° for **1** and 109.2(4)–109.8(5)° for **2**. All these results indicate that the $[PMo_{12}O_{40}]^{3-}$ units have a normal Keggin structure in the polymeric-polyanion chains. The poly-Keggin-type anions play not only a charge-compensating role, but they can dramatically influence the overall solid-state architecture through their templating function, as well as the cationic framework with special channels also influences the polymerization of polyanions through its host function. In addition, several hydrogen bonds exist between the polyanion chain and the channel, such as between the water molecules O(2 W) and O(4 W) belong to the $[M(H_2O)_8]^{2+}$ clusters and O(9) and O(12) centers of the polyanions, as well as between water molecules O(5 W) in the $H^+(H_2O)_m$ clusters and O(11) centers of the polyanions. As a result, based on self-assembly of HINO molecules, $[M(H_2O)_8]^{2+}$ and $H^+(H_2O)_m$ clusters, both complexes form 3D H-bonding networks with 1D channels along the *a*-axis, in which polyanions chains were formed and stabilized based on electrostatic and H-bonding interactions, resulting in $[PMo_{12}O_{40}]^{3-}$ anions being not easy dissociated from the hybrid networks. Moreover, the section size of the channels along the *b* and *c* axes is so larger than the diameter of the $[PMo_{12}O_{40}]^{3-}$ anion (ca. 10.4 Å), that there is enough space outside the polyanion chains to admit some small species, such as water molecules or hydronium ions, to transport along the channels. All these results indicate that **1** and **2** can potentially be new highly proton-conducting materials.

3.2. TG analysis

These complexes are insoluble in water. Water retention in the hybrid at high temperature is a key factor for having fast protonic conduction [3,4]. Thermogravimetric analyses of the powder of the crystalline samples of two complexes in an atmosphere of N_2 (Fig. 5) both show no weight loss in the temperature range of 20–100 °C, indicating that all water molecules in the unit structure are involved in constructing the H-bonding network, which is consistent with the result of structural analysis, and are not easily lost below 100 °C. This is not like that observed in the proton conductors including the quasi-liquid water clusters (which are generally loosely bonded in the structure) like a Nafion membrane [13] and pure tungstophosphoric acid (PWA-26) or molybdophosphoric acid (PMA-26) [1,2].

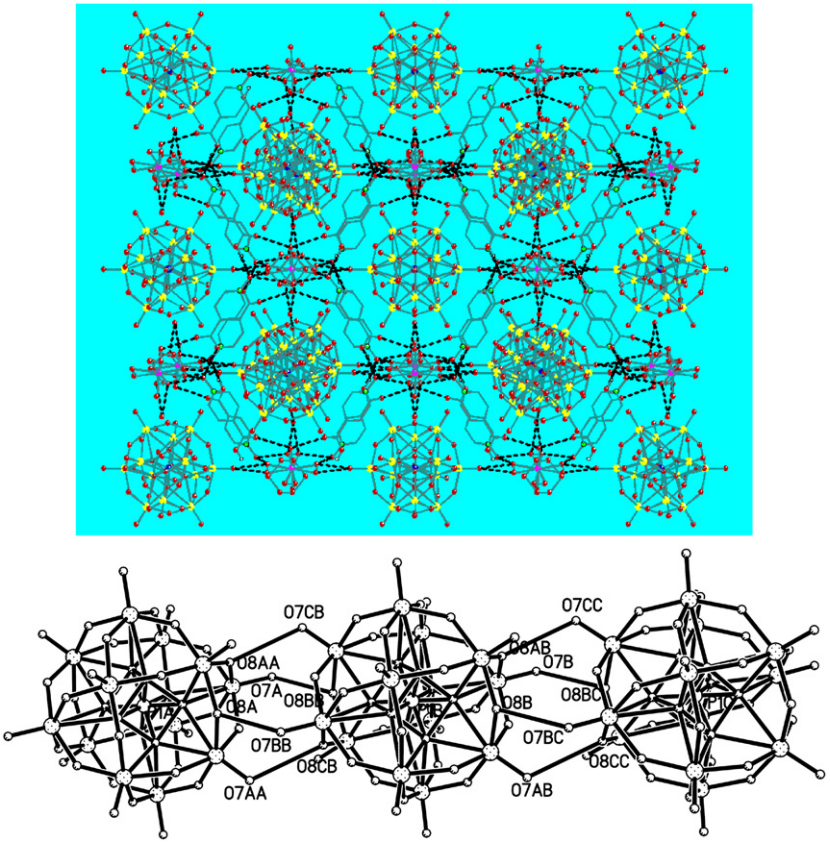

Fig. 4. Representative 3D hydrogen-bonded network showing the 1D channels filled by polyanion chains down the *a*-axis (top), and view of the polyanion chain along the *a*-axis (bottom). Zn(Mn), N, O, Mo and P are represented as purple, green, red, yellow and blue, respectively. Hydrogen atoms are omitted for clarity. Selected atom···atom distances (Å) for complex **1**: O(2 W)···O(12 A) 2.794(2), O(4 W)···O(9) 2.916(2), O(6 W)···O(11B) 3.356(3); for complex **2**: O(2 W)···O(12 A) 2.800(2), O(4 W)···O(9) 2.922(2), O(6 W)···O(11B) 3.167(3). Symmetry code: A, $-x+3/2$, $y+1/2$, $-z+1/2$; B, $-x+1$, $-y$, z. (For interpretation of the references to color in this figure legend, the reader is referred to the web version of this article.)

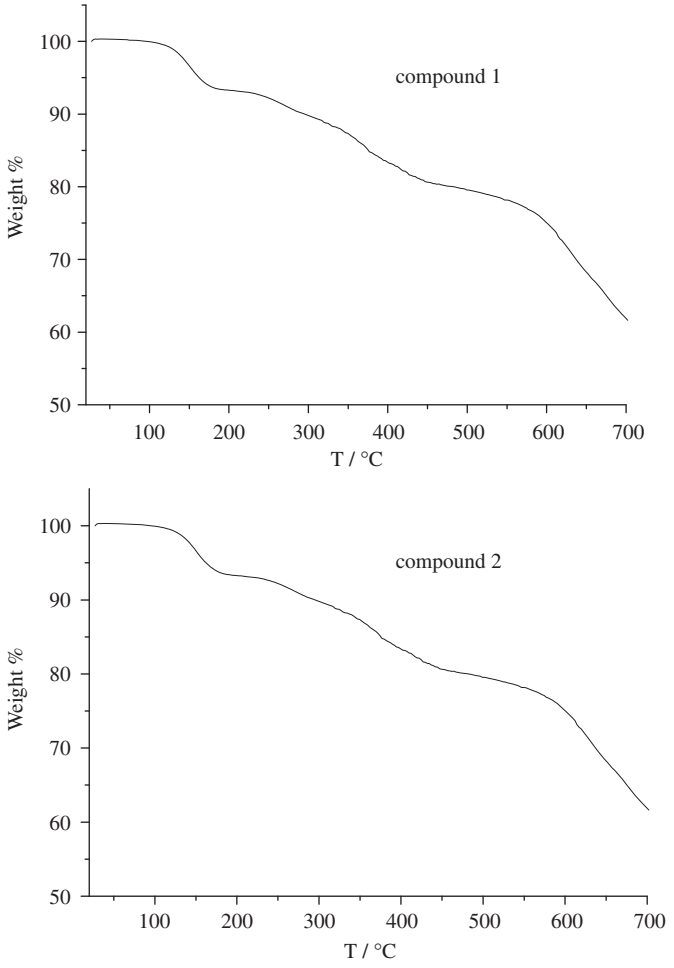

Fig. 5. Curves of the Perkin-Elmer thermal analyses of complexes **1** and **2** in the atmosphere of N_2.

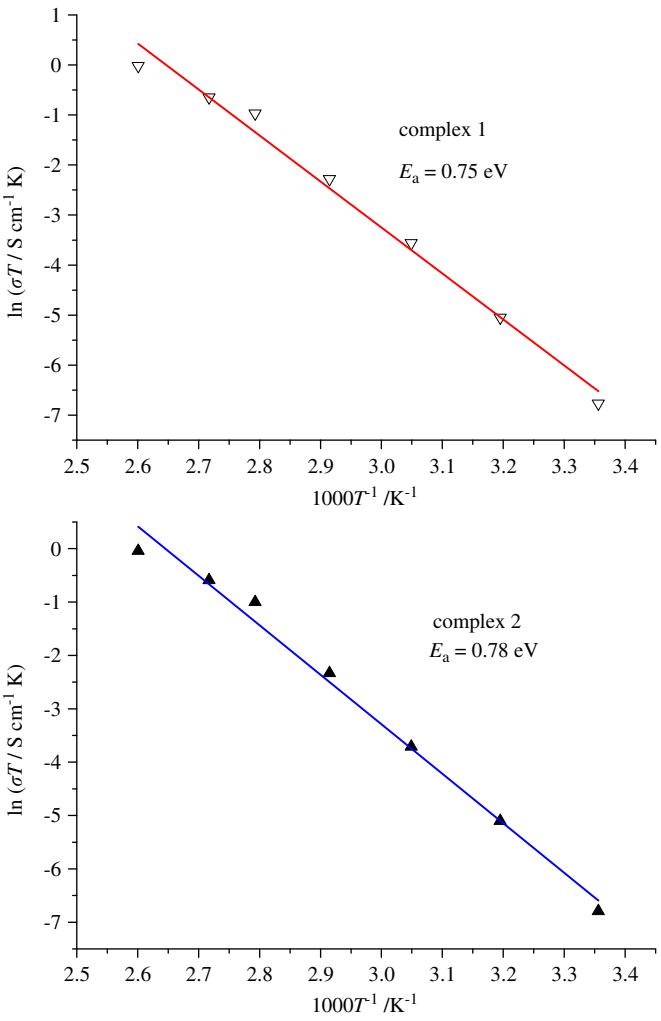

Fig. 6. The Arrhenius plots of the proton conductivities of complexes **1** and **2.**

3.3. Proton conductivity

The proton conductivities of **1** and **2** in the temperature range of 25–100 °C were therefore evaluated by the ac impedance method using a compacted pellet of the powdered crystalline sample. At 25 °C, both complexes showed poor proton conductivities of $\sim 9.0 \times 10^{-9}$ S cm^{-1} under 35% RH conditions, estimated from the Nyquist plots shown in the Supplementary information, but their proton conductivities reached $\sim 4.0 \times 10^{-6}$ S cm^{-1} with RH up to 98%. Again, we measured their ionic conductivities up to 100 °C under 98% RH conditions. Surprisingly, both complexes reached high proton conductivities of $1.44–2.85 \times 10^{-3}$ S cm^{-1} in the temperature range of 85–100 °C. These proton conductivities are comparable to Nafion, which is in practical use in fuel cells [13].

Fig. 6 shows the Arrhenius plots of the proton conductivities of two complexe**s** in the temperature range of 25–100 °C under 98% RH conditions. The ln σT increases almost linearly with temperature range from 25 to 100 °C, and the corresponding activation energy (E_a) of conductivity was estimated to be 0.75 eV for **1** and 0.78 eV for **2** from the equation below.

$$\sigma T = \sigma_0 \exp(-E_a/k_B T) \quad (1)$$

where σ is the ionic conductivity, σ_0 is the pre-exponential factor, k_B is the Boltzmann constant, and T is the temperature. Both E_a values are very high. The results show that the general features of the changes in conductivities are different from that of protonic conducting polymer membrane such as Nafion, which has almost identical protonic conductivity over a wide temperature range from ambient to 100 °C with activation enthalpy of approximately 0.15 eV, when it is fully humidified [13]; and are different from that of PWA-26 or PMA-26, whose protonic conductivity decreased with the temperature from ambient to 60 °C [1,2]. However, the title complexes have thermally activated protonic conductivities [12b] from 25 to 100 °C; as the temperature increases, the proton conductivities increase on a logarithmic scale even with almost saturated humidities. This is probably due to the fact that protons belong to the protonated water clusters and those originating from water molecules need a thermally activated process for dissociation as hydrated forms such as H^+, H_3O^+ or other proton species at a distance from $[PMo_{12}O_{40}]^{3-}$ clusters [14]. The mechanism of proton conduction of **1** and **2** is, therefore, expected to be similar to that of the vehicle mechanism [15], that is, the direct diffusion of additional protons with water molecules. As shown in Fig. 4, the section size of the channels along the *b* and *c* axes is so larger than the diameter of the $[PMo_{12}O_{40}]^{3-}$ anion (ca. 10.4 Å), that there is enough space outside the polyanion chains to admit some small species, such as water molecules or hydronium ions, to transport along the channels. In addition, the existence of these half- or quarter-occupied oxygen sites of water molecules in $[M(H_2O)_8]^{2+}$ and $H^+(H_2O)_m$ clusters may be conducive to the forming of the H-bonding network and to the proton transport along the H-bonding network [16]. As shown in Figs. 3 and 4, the existence of H-bonding networks suggests that proton conduction in two

complexes includes some other process such as proton transport of additional protons along H-bonding networks (Grotthus mechanism) [17].

It is possible that in higher temperature and humidity some of isonicotinic acid N-oxide molecules can be deprotonated and the protons can be incorporated by the water molecules and therefore conductivity can be a result of dissociation of organic acid. The results of measurement of the proton conductivity of HINO molecules in the temperature range of 85–100 °C at 98% RH showed the free HINO molecules reached proton conductivities of 10^{-5}–10^{-4} S cm^{-1} in the temperature range of 85–100 °C (see supplementary material), these proton conductivities are about 1–2 orders of magnitude lower than that of the title complex, which shows conductivity of about 10^{-3} S cm^{-1} in the conditions described. Therefore, the fact that the title complex exhibits good proton conductivities in the temperature range of 85–100 °C is indicative of a high carrier concentration based on a thermally activated process, as well as the existence of the whole H-bonding networks. Moreover, there is the possibility of hydrolysis of the complexes when they are held at 100 °C with a RH higher than 98% (100%, or condensed water that attack the metal centers). The powder X-ray diffraction data in the Supplementary materials suggested that the powder samples after the proton-conductive measurement have the same supramolecular frameworks as those of complexes **1** and **2**.

Interestingly, for complexes **1** and **2**, though the M^{2+} ion is different, they have the similar 3D H-bonding networks and the proton conductivities, suggesting that Zn^{2+} and Mn^{2+} ions could form similar ionized water cluster and that the origin of proton conduction in these complexes is based on the self-ordered H-bonding structure and the polyanion chains.

4. Conclusion

Two highly proton-conductive organic–inorganic complexes have been constructed by introducing Keggin-type polyanions as countercations and templates into the cationic H-bonding networks formed by ionized water clusters and HINO molecules. The organic–inorganic hybrid matrix changed the environment around transition metal salts of HPAs and influenced the formation of poly-Keggin anions within the resultant structure. Thus, these complexes provide a new route in increasing the stability and proton conductivity of organic–inorganic hybrid materials based on salts of HPAs at high temperature, as well as may become a new type of proton conducting additives in proton exchange composite membranes for use under dry and/or elevated temperature conditions of fuel cell.

Supplementary information

CCDC-800902 (for **1**) and -800903 (for **2**) contain the supplementary crystallographic data for this paper. These data can be obtained free of charge from The Cambridge Crystallographic Data Center via www.ccdc.cam.ac.uk/data_request/cif. The Nyquist plots for two complexes at 25–100 °C under 98% relative humidity.

Acknowledgments

This work was supported by the National Natural Science Foundation of China (20971038), the Natural Science Foundation of the Education Department of Henan Province (2009A150015), the Science Foundation for Youths of Henan Normal University (2008qk10) and undergraduate innovative pilot scheme of Henan Normal University (2009050).

Appendix A. Supporting materials

Supplementary data associated with this article can be found in the online version at doi:10.1016/j.jssc.2011.04.025.

References

[1] (a) O. Nakamura, T. Kodama, I. Ogino, Y. Miyake, Chem. Lett. (1979) 17;
(b) M. Misono, Chem. Commun. (2001) 1141;
(c) R.C.T. Slade, J. Barker, H.A. Pressman, J.H. Strange, Solid State Ionics 28 (1988) 594;
(d) D.E. Katsoulis, Chem. Rev. 98 (1998) 359;
(e) J.L. Malers, M.A. Sweikart, J.L. Horan, J.A. Turner, A.H. Herring, J. Power Sources 172 (2007) 83;
(f) A.M. Herring, Polym. Rev. 46 (2006) 245.
[2] (a) G. Alberti, M. Casciola, Solid State Ionics 145 (2001) 3;
(b) G. Alberti, M. Casciola, U. Costantino, A. Peraio, T. Rega, J. Mater. Chem. 5 (1995) 1809;
(c) X.G. Sang, Q.Y. Wu, W.Q. Pang, Mater. Chem. Phys. 82 (2003) 405;
(d) I. Honma, S. Nomura, H. Nakajima, J. Membr. Sci. 185 (2001) 83;
(e) J.D. Kim, I. Honma, Solid State Ionics 176 (2005) 547.
[3] (a) B. Tazi, O. Savadogo, Electrochim. Acta 45 (2000) 4329;
(b) Y.S. Kim, F. Wang, M. Hickner, T.A. Zawodzinski, J.E. McGrath, J. Membr. Sci. 212 (2003) 263;
(c) I.V. Kozhevnikov, J. Mol. Catal. A: Chem 262 (2007) 86;
(d) J.L. Malers, M.A. Sweikart, J.L. Horan, J.A. Turner, A.H. Herring, J. Power Sources 172 (2007) 83.
[4] (a) V. Ramani, H.R. Kunz, J.M. Fenton, J. Membr. Sci. 232 (2004) 31;
(b) A.M. Herring, Polym. Rev. 46 (2006) 245;
(c) G. Inzelt, M. Pineri, J.W. Schultze, M.A. Vorotyntsev, Electrochim. Acta 45 (2000) 2403;
(d) A. Verma, K. Scott, J. Solid State Electrochem. 14 (2010) 213.
[5] (a) J. Lu, F.X. Xiao, L.X. Shi, R. Cao, J. Solid State Chem. 181 (2008) 313;
(b) Z.G. Han, Y.L. Zhao, J. Peng, H.Y. Ma, Q. Liu, E.B. Wang, N.H. Hu, J. Solid State Chem. 177 (2004) 4325;
(c) J.D. Kim, I. Honma, Solid State Ionics 176 (2005) 547.
[6] R.D. Claude, F. Michel, F. Raymonde, T. Rene, Inorg. Chem. 22 (1983) 207.
[7] P.G. Simapson, A. Vinciguerra, J.V. Quagliano, Inorg. Chem. 2 (1963) 282.
[8] Q.Y. Wu, S.L. Zhao, J.M. Wang, J.Q. Zhang, J Solid State Electrochem. 11 (2007) 240.
[9] SMART and SAINT, Area Detector Control and Integration Software, Siemens Analytical X-ray Systems, Inc., Madison, WI, 1996.
[10] G.M. Sheldrick., SHELXTL Version 5.1), Software Reference Manual, Bruker AXS, Inc., Madison, WI, 1997.
[11] (a) M.L. Wei, C. He, Q.Z. Sun, Q.J. Meng, C.Y. Duan, Inorg. Chem. 46 (2007) 5957;
(b) M.L. Wei, C. He, W.J. Hua, C.Y. Duan, S.H. Li, Q.J. Meng, J. Am. Chem. Soc. 128 (2006) 13318;
(c) C.Y. Duan, M.L. Wei, D. Guo, C. He, Q.J. Meng, J. Am. Chem. Soc. 132 (2010) 3321;
(d) M.L. Wei, H.Y. Xu, R.P. Sun, J. Coord. Chem. 62 (2009) 1989;
(e) M.L. Wei, P.F. Zhuang, H.H. Li, Y.H. Yang, Eur. J. Inorg. Chem. (2011) 1473.
[12] (a) Y. Kanda, K.Y. Lee, S. Nakata, S. Asaoka, M. Misono, Chem. Lett. (1988) 139;
(b) J. Yang, M.J. Janik, D. Ma, A. Zheng, M. Zhang, M. Neurock, R.J. Davis, C. Ye, F. Deng, J. Am. Chem. Soc. 127 (2005) 18274.
[13] (a) K.D. Kreuer, S.J. Paddison, E. Spohr, M. Schuster, Chem. Rev. 104 (2004) 4637;
(b) R.C.T. Slade, A. Hardwick, P.G. Dickens, Solid State Ionics 9 (1983) 1093;
(c) G. Alberti, M. Casciola, Solid State Ionics 145 (2001) 3.
[14] (a) M.J. Janic, R.J. Davis, M. Neurock, J. Am. Chem. Soc. 127 (2005) 5238;
(b) E.G. Hayashi, J.B. Moffat, J. Catal. 83 (1983) 192;
(c) I. Honma, S. Nomura, H. Nakajima, J. Membr. Sci. 185 (2001) 83.
[15] K.D. Kreuer, A. Rabenau, W. Weppner, Angew. Chem., Int. Ed. 21 (1982) 208.
[16] (a) M. Sadakiyo, T. Yamada, H. Kitagawa, J. Am. Chem. Soc. 131 (2009) 9906;
(b) W.A. England, M.G. Cross, A. Hamnett, P.J. Wiseman, J.B. Goodenough, Solid State Ionics 1 (1980) 231.
[17] N. Agmon, Chem. Phys. Lett. 244 (1995) 456.